International Journal of Pressure Vessels and Piping 89 (2012) 151–161

Contents lists available at SciVerse ScienceDirect

International Journal of Pressure Vessels and Piping

journal homepage: www.elsevier.com/locate/ijpvp

An engineering assessment methodology for non-sharp defects in steel structures – Part II: Procedure validation and constraint analysis

A.J. Horn [a,*], A.H. Sherry [b]

[a] Tata Steel Research Development and Technology, Swinden Technology Centre, Moorgate, Rotherham S60 3AR, UK
[b] Dalton Nuclear Institute, University of Manchester, Sackville Street, Manchester M60 1QD, UK

ARTICLE INFO

Article history:
Received 24 February 2011
Received in revised form
27 September 2011
Accepted 11 October 2011

Keywords:
Fracture toughness
Cleavage fracture
Crack
Notch
Constraint

ABSTRACT

This Part II paper validates a new engineering methodology for assessing non-sharp defects in ferritic steel structures. The new approach, presented in the companion Part I paper, is based on a modification of the Failure Assessment Diagram for notches. A series of worked examples is presented based on a large dataset of U-notched SE(B) specimens machined from a heat-treated structural steel grade S690. Failure predictions of notched specimens using the modified approach result in significantly reduced conservatism compared to the standard Failure Assessment Diagram assessment method. The new methodology is also combined with the existing constraint-modified approach in the R6 defect assessment method to predict cleavage fracture in shallow, blunt-notched SE(B) specimens with a small degree of conservatism.

1. Introduction

Structural integrity assessments are often carried out in the context of a Failure Assessment Diagram (FAD) that provides a graphical representation of the degree to which fracture and plastic collapse contribute to structural failure. The abscissa L_r indicates the proximity to failure by plastic collapse and is defined by the applied load P normalised by the plastic limit load P_L. The ordinate K_r indicates the proximity to fracture. K_r is defined by the ratio of the linear elastic stress intensity factor K_I to the material toughness K_{mat}. K_r and L_r are both proportional to P and a linear loading line can be plotted on the FAD. Failure is predicted at its intersection with the failure assessment curve, represented by the equation:

$$K_r = f(L_r) \text{for} \quad L_r < L_r^{max} \tag{1}$$

where L_r^{max} is the ratio of the uniaxial flow stress to the uniaxial yield stress σ_y defined at 0.2% plastic strain where flow stress is defined as the mean of the ultimate tensile stress (UTS) and σ_y.

Current FAD procedures usually assume flaws to be infinitely sharp: while this assumption may be appropriate for fatigue cracks, in other cases such as elongated voids or mechanical dents this can be an over-conservative assumption that can lead to pessimistic assessment of structures and significant under-estimation of their safety margin against fracture. Structures containing blunt notches instead of cracks exhibit higher values of effective toughness compared to sharp cracks [1–11]. In an attempt to take advantage of the increased effective toughness associated with a notch, a new FAD-based engineering assessment methodology is proposed in the companion Part I paper [12]. The modification of the FAD for non-sharp defects can be applied irrespective of failure mechanism. The main benefit arises from the increase in effective toughness with increasing notch radius. Although this benefit appears whether the initiating failure mechanism is cleavage or ductile tearing, these papers focus on cleavage fracture. Several parameters are required in order to modify the FAD for non-sharp defects: the notch driving force is described by the notch J-integral J^ρ, the notch tip loading severity by the elastic notch tip opening stress σ_N, the notch geometry by a load-independent parameter β_N, and the sensitivity of the material toughness to the notch effect by the non-dimensional material parameters γ and l. These material parameters can either be measured by testing notched specimens of the same thickness as the structure, or for cleavage fracture they can be obtained using look-up tables generated using the Weibull stress toughness scaling model. The other parameters in the procedure can either be conservatively estimated using simple equations (called the “basic option”) or they can be determined more accurately using finite element analysis (termed the “FE option”).

* Corresponding author.
E-mail address: Anthony.J.Horn@tatasteel.com (A.J. Horn).

0308-0161/$ – see front matter © 2011 Elsevier Ltd. All rights reserved.
doi:10.1016/j.ijpvp.2011.10.015

The proposed methodology is presented in detail in Section 3 of the companion Part I paper [12].

1.1. Objective and structure of paper

The objective of this Part II paper is to describe the validation of the new FAD-based assessment method for non-sharp defects proposed in the companion Part I paper [12] and summarised above. This is performed with respect to a large database of single edge notch bend SE(B) specimens containing a range of deep and shallow cracks and blunt notches. The paper is structured as follows. Section 2 describes a series of deeply cracked and notched SE(B) specimens which are subsequently evaluated using the notch-based FAD in Section 3. The interaction of the notch and constraint effects are investigated in Section 4. The results of a combined notch and constraint-corrected FAD analysis is described in Section 5 and compared with test data on shallow blunt-notched SE(B) tests. A discussion is provided in Section 6 and conclusions presented in Section 7.

2. Deeply notched SE(B) tests with notches

2.1. Material

The material used for the study was a 35 mm thick roller-quenched and tempered structural steel grade S690Q. It is used in the construction industry and has a minimum specified yield stress of 690 MPa and an ultimate tensile strength in the range 790–930 MPa.

The normal microstructure for this grade of steel is tempered martensite to achieve combined high strength and high fracture toughness. In order to raise the fracture toughness transition temperature and avoid the need for performing tests at low temperatures, the plate was austentized by heating to 1100 °C for 2½ hours. This was followed by furnace cooling to 650 °C and air-cooling to room temperature to produce a coarse ferrite-pearlite microstructure with martensitic islands. More details of this material are provided in reference [9].

2.2. Specimen geometry

A large test programme was undertaken comprising 60 SE(B) specimens containing cracks or notches of differing radii. All specimens were machined 2 mm sub-surface, oriented longitudinally, notched in the transverse direction (i.e. X–Y and L-T orientation according to the notations of [13] and [14] respectively) and had thickness B and width W equal to 12.5 mm. Pre-cracking of the standard SE(B) specimens was performed at ambient temperature to a nominal crack depth, a_0, to specimen width ratio $a_0/W = 0.5$. Precise values of pre-crack length a_0 were measured using a nine-point average after testing.

Specimens containing blunt notches instead of fatigue pre-cracks were prepared by machining a semi-circular notch of radius ρ to a nominal depth of 6.25 mm ($a_0/W = 0.5$), Fig. 1. Five values of ρ were machined: 0.16 mm, 0.25 mm, 0.75 mm, 1.2 mm and 2.0 mm, corresponding to $\rho/a_0 = 0.03$, 0.04, 0.12, 0.19 and 0.32 respectively. For specimens with $\rho/a_0 = 0.19$ and 0.32, the notches were machined using a cutting wheel; all other notch radii were machined using electro-discharge machining. Values of a_0 were calculated as the mean of two notch length measurements made on the front and back face of each specimen prior to testing.

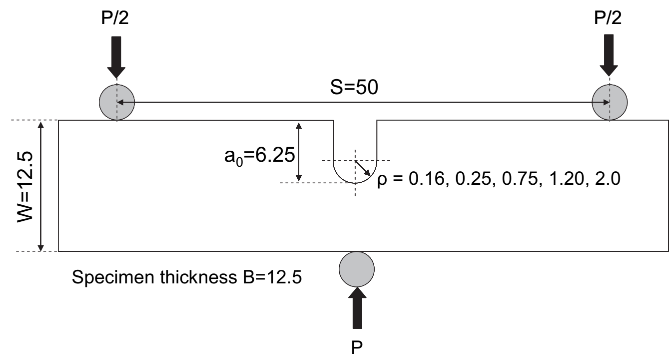

Fig. 1. Geometry of SE(B) specimens tested, all dimensions in mm.

2.3. Test procedure

All specimens were tested in three-point bending at 0 °C with span $S = 4W = 50$ mm and a double clip gauge arrangement above the crack mouth as specified in [13]. Tests were carried out in an environmental chamber with the specimen temperatures monitored using a thermocouple spot welded to the surface of the specimen and located less than 2 mm ahead of the crack tip. All specimens were held at the test temperature for at least 13 min (1 min per millimetre of specimen thickness) prior to testing. Specimens were loaded until failure occurred by cleavage fracture or just following maximum load. Initial loading rates in the elastic regime were between 0.15 and 0.20 kNs^{-1}.

For each notch radius, validated finite element models (described in [9]) were used to establish the relationship between load-line displacement (LLD) and clip gauge opening. Although the relationships were approximately linear, sixth order polynomials provided the most satisfactory fit. These were used to calculate two values for each test specimen (one for each clip gauge), the mean of which defined the LLD.

An effective J for all cracked and notched SE(B) specimens was then derived from the load vs. LLD trace using the expression provided in ESIS P2-92 [15]:

$$J^{\rho}_{LLD} = \frac{\eta^{LLD} U^{LLD}}{B(W - a_0)} \quad (2)$$

where $\eta^{LLD} = 2.0$, U^{LLD} is the total area under the load vs. load-line displacement trace, B and W are the specimen thickness and width respectively ($B = W = 12.5$ mm) and a_0 is the crack or notch length. The ESIS method of calculating J was used because this provides a more accurate estimation of the J-integral for notched SE(B) specimens [12] than partitioned expressions such as those in ASTM E1820-08a or BS7448-1.

2.4. Experimental results

The test results are shown in Fig. 2, plotted as J^{ρ}_{LLD} vs. ρ/a_0. Specimens with low values of ρ failed suddenly at low values of J during a rising load. Examination of the fracture surfaces confirmed failure occurred by cleavage fracture [9]. Specimens with higher values of ρ/a_0 failed at higher values J indicating an increasing amount of energy is required to initiate cleavage fracture with increasing ρ. For large values of notch tip radius ($\rho/a_0 \geq 0.19$), some specimens reached maximum load, indicated by squares in Fig. 2. Thereafter, a reduction in applied load was observed. Examination of such specimens after testing revealed the presence of ductile tearing at the notch tip.